1

Design of an Assistive Gait Device for Strength Endurance and Rehabilitation

K. H. Low[1], Xiaopeng Liu[1] and Haoyong Yu[2]
[1]*School of MAE, Nanyang Technological University*
[2]*Dept. of ME, National University of Singapore*
Singapore

1. Introduction

1.1 Background

Exoskeletons for human performance augmentation (EHPA) are controlled and wearable devices and machines that can increase the speed, strength, and endurance of the operator. EHPA is expected to do that by increasing the physical performance of the solider wearing it, including:

- Increased payload: more fire power, more supplies, and thicker and heavier armor increasing the soldier chance of surviving a direct hit or even an explosion.
- Increased speed and extended range: enhanced ground reconnaissance and battle space dominance.
- Increased strength: larger caliber weapons, obstacle clearance, repairing heavy ma chinery such as tack.

Besides these, "Imagine the psychological impact upon a foe when encountering squads of seemingly invincible warriors protected by armor and endowed with superhuman capabilities, such as the ability to leap over 20-foot walls, " said Ned Thomas, the director of Institute for Soldier Nanotechnologies (ISN) (Wakefield, 2002). Another use of exoskeletons is that they could help integrate women into combat situations. John Knowles, publisher of the defense industry newsletter, The Knowles Report, said that in terms of marksmanship and other combat skills, "Women have proven themselves very equal." The prevailing argument against women in combat is that most can't meet the job's physical requirements. Exoskeletons, could "radically equalize that," thus enabling a 130-pound woman to lift, carry and be as effective as a 180-pound man (Hembree, 2001). In non-military areas, one of the most possible applications of exoskeletons may be used to help aged or disabled people whose lower extremities have locomotor deficiencies due to various reasons: polio, paraparesis, paralysis, dystrophia, etc. They are unable to walk without assistance and may lose muscular strength in their legs and become bedridden. They can only move around by a wheelchair or by using a wheeled walker. Unfortunately, barriers such as bumps and steps restrict the area that these people have access to. It is hoped that the lower exoskeleton can enhance their muscular strength and enable them walk as normal people.

Source: Humanoid Robots: Human-like Machines, Book edited by: Matthias Hackel
ISBN 978-3-902613-07-3, pp. 642, Itech, Vienna, Austria, June 2007

1.2 Objective and Scopes

In light of the recent surge of interest in exoskeletons, much research has been devoted to developing exoskeleton systems. However, most of these studies only focus on upper extremity exoskeletons, which are ground based. Lacking the locomotion capabilities for walking with the user, their application is inevitably limited. With fund from Ministry of Defense, Singapore, we are considering to develop a lower extremity exoskeleton (LEE). The LEE is aiming to help the user carry heavy loads by transferring the load weight to the ground (not to the wearer). It could provide soldiers the ability to carry heavy loads such as food, communications gear, and weaponry, without the strain typically associated with demanding labor. We also hope with improvements it might provide a versatile transport platform for mission-critical equipment. The scopes of the present work are:

- Study and examination of the key technologies required to successfully build an ex oskeleton
- Investigation of the control strategy and the exoskeleton to user interface
- Design and construction of an experimental prototype
- Implementation of the control algorithm on the constructed prototype
- Realization of normal walking

2. Literature Review

Exoskeleton has been an active field of research in recent years (Guizzo & Goldstein, 2005). This section briefly describe some exoskeleton systems and assistive devices developed around the world.

2.1 UC Berkeley's Exoskeletons

In 2000, the Defense Advanced Research Projects Agency (DARPA) launched a program over five years on developing EHAP to give infantry soldiers an extra edge *(Exoskeletons for Human Performance Augmentation Projects,* 2002). One of the facilities that received the research founds from DAPRA is located at the UC Berkeley.

In 2004, Berkeley Lower Extremity Exoskeleton (BLEEX) was first unveiled. The BLEEX is designed to have the same degrees of freedom similar to those of the pilot: three degrees at the ankle and the hip, and one degree at the knee. However, it is hydraulically actuated only at the hips, knees and ankles to allow flexion and extension of the hip joints and knee joints as well as dorsiflexion and plantarflexion of the ankle joints. The other non-actuated degrees of movements are then spring loaded to a default standing posture. The exoskeleton connects to the user at the foot by strapping onto the user's boots. A bendable sole allows for bending of the users toes; and ankle abduction and vertical rotation are allowed for better flexibility. A torso connects the user's back and hips to the exoskeleton legs. A full-body vest is incorporated onto the torso to avoid discomfort or abrasion to the user. The BLEEX employs a high-tech compact Hydraulic Power Unit (HPU). The stand-alone hybrid power source is able to deliver hydraulic power for actuation and electric power for the computers and sensors for long hours. The HPU is the synthesis of a gasoline engine, a three-phase brushless generator and a hydraulic gear pump. Exclusive designing by UC Berkeley enables the HPU to regulate the hydraulic pressure and engine speed via an engine throttle and a hydraulic valve. This unique employment of power supply enables the BLEEX to operate more efficiently and lightweight for a longer period of time. The control scheme

needs no direct measurements from the pilot or the human-machine interface, instead, the controller estimates, based on measurements from the exoskeleton only. The basic principle for the control of BLEEX rests on the notion that the exoskeleton needs to shadow the wearers voluntary and involuntary movements quickly, and without delay (Kazerooni, Racine, Huang, & Steger, 2005). This requires a high level of sensitivity in response to all forces and torques on the exoskeleton. However, an exoskeleton with high sensitivity to external forces and torques would respond to other external forces not initiated by its pilot, the pilot would receive motion from the exoskeleton unexpectedly and would have to struggle with it to avoid unwanted movement. The other concern is that systems with high sensitivity to external forces and torques are not robust to variations and therefore the precision of the system performance will be proportional to the precision of the exoskeleton dynamic model. Hence the model accuracy is crucial to exoskeleton control. The dynamics of the exoskeleton should be understand quite well and the controller is heavily model based. In together, that maximizing system sensitivity leads to a loss of robustness in the system. However, inventive or state-of-the-art the BLEEX may sound, actual videos of tests done on the BLEEX shows certain drawbacks. First of all, the user seemed hampered and unnatural during walking. Also, the backpack looks bulky and makes the whole system rather unbalanced. The costs of building a BLEEX prototype were also not mentioned by the developers. One would suspect that such a complex system, especially with its high-tech HPU, would cost quite considerably.

Figure 1. BLEEX prototype *(Berkeley Robotics Laboratory,* Dec. 2004)

2.2 Assistive Devices

Many institutions around the world have carried out research and development on exoskeletons and assistive devices to empower or aid the human limbs. Yobotics Incorporation's RoboKnee *(Robo Walker,* Dec. 2003), Japan's hybrid assistive limbs (HAL) *(Powered Suit HAL (Hybrid Assistive Leg),* Dec. 2003), Northeastern University's Active Knee Rehabilitation Device (AKROD) (Mavroidis, 2005) are some of the leading developments in the area of assistive devices to aid the human limb.

2.3 RoboWalker

Figure 2. RoboKnee developed by Yobotics, Inc. *(RoboWalker,* Dec. 2003)

To help people who are suffering from weakness in their lower extremities, Yobotics, Inc., is developing a powered, wearable device called the RoboWalker. The RoboWalker augments or replaces muscular functions of the lower extremities. In 2001, they produced a prototype powered knee orthotic, called the RoboKnee, shown in Figure 2. With the computer, amplifiers, and batteries in a backpack, while not super impressive, the RoboKnee did provide for super-human capabilities by allowing the user to perform deep knee bends almost indefinitely. According to their homepage *(RoboWalker,* Dec. 2003), they are still looking for funds for the next stage of development.

2.4 Hybrid Assistive Leg

As shown in Figure 3, Hybrid Assistive Leg (HAL) (Kasaoka & Sankai, 2001; Kawamoto & Sankai, 2002; Tomohiro Hayashi & Sankai, 2005) is an exoskeleton type power assist system developed by Tsukuba University to realize the walking aid for aged people or gait-disorder persons.

2.5 AKROD

The AKROD-v2 (Mavroidis, 2005) developed by the Northeastern University consists of a robotic knee brace that is portable and programmable. As shown in Figure 4, the device contains electro-rheological fluid on one side of its structure such that it can turn solid in less than a millisecond with the application of a voltage. This would provide resistance to motion on a healing joint and it aims to help the muscle regain strength. The purpose of this device is to retrain the gait of a stroke patient.

Figure 3. HAL-3 developed by Japan's Tsukuba University *(Powered-suit gives aged a leg up,* Dec. 2003)

2.6 NTU Assistive Device

For the purpose of assisted walking, another prototype with the footpad design, as shown in Figure 5, has bee developed and tested for the walking and stair-climbing (Low & Yin, 2007).

Figure 4. Northeastern University's AKROD (*Mavroidis*, 2005)

Figure 5. NTU's Assistive Device (*Low & Yin*, 2007)

3. Gait Dynamics

Biped locomotion has been at the focus of researchers for decades. It is well known that biped gait can be divided into two phases: *single support phase* and *double support phase* (Whittle, 1991). In the single support phase, one leg is moving in the air, while the other leg is in contact with the ground. In the double support phase, both feet are with contact with the ground. The two support phases take place in sequence during walking. All of the biped mechanism joints are powered and directly controllable, except for the contact area between the foot and the ground. Foot behavior cannot be controlled directly, it is controlled indirectly by ensuring appropriate dynamics of the mechanism above the foot. To account for this, the concept of zero moment point (ZMP) (Vukobratović & Juricic, 1969), which is denned as the point on the ground at which the net moment of the inertial forces and the gravity forces has no component along the horizontal axes, has been used. The gait is balanced when and only when the ZMP trajectory remains within the support area. In this case, the system dynamics is perfectly balanced by the ground reaction force and overturning will not occur. In the single-support phase, the support polygon is identical to the foot surface. In the double support phase, however, the size of the support polygon is denned by the size of the foot surface and by the distance between them (the convex hulls of the two supporting feet).

The ZMP concept provides a useful dynamic criterion for the analysis and synthesis of biped locomotion. The ZMP ensures the gait balance during the entire gait cycle and provides a quantitative measure for the unbalanced moment about the support foot and for the robustness (balancing margin) of the dynamic gait equilibrium. Another term is center of pressure (CoP) (Vukobratović, Borovać, Šurdilović, & Stokić, 2001), which is commonly

used in biped gait analysis based on force or pressure measurements. CoP represents the point on the support foot polygon at which the resultant of distributed foot ground reaction force acts. According to their definitions, it is obviously that in the considered single-support phase and for balanced dynamic gait equilibrium, the ZMP coincides with the CoP. However, in the dynamically unbalanced single-support situation that is characterized by a moment about CoP that could not be balanced by the sole reaction forces, the CoP and the ZMP do not coincide. The ZMP location outside the support area provides useful information for gait balancing (Low, Liu, Goh, & Yu, 2006). The fact that ZMP is instantaneously on the edge or outside of the support polygon indicates the occurrence of an unbalanced moment that cannot be compensated for by foot reaction forces. The distance of ZMP from the foot edge provides the measure for the unbalanced moment that tends to rotate the biped around the supporting foot and, possibly, to cause a fall. As depicted in Figure 6, the exoskeleton is composed of the trunk, the pelvis, two shanks, two thighs and two feet, will be considered. The trunk carries the payload, which can be seen as a part of the trunk. The vertical Z-axis and horizontal *X*-axis lie in the sagittal plane, as shown in Figure 6. By observing typical human joint trajectories, it is noted that the motion range is greater in sagittal plane than in other planes (Marchese, Muscato, & Virk, 2001) and most movements happen in the sagittal plane during walking. Hence, at the first stage, only the joints rotating around the Y-axis are actuated and movements in the sagittal plane are studied. The dynamical equation that describes the movement of a biped (or exoskeleton) has the following form:

$$M(\vec{q})\ddot{\vec{q}} = f(\vec{q}, \dot{\vec{q}}) + \vec{Q} \tag{1}$$

where $\vec{q} = (q_1, ..., q_7)^T$ is the vector of generalized coordinates, which are the joint angles.

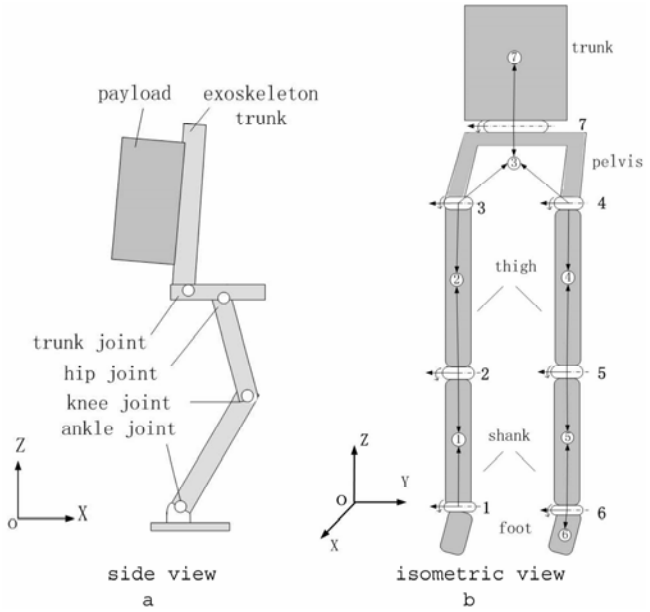

Figure 6. The model of the exoskeleton

The matrix function $M(\vec{q})$ takes into account the mass distribution, and the vector function $f(\vec{q},\dot{\vec{q}})$ describes the effect of both inertial and gravity forces. The elements of the vector $\vec{Q}$ are generalized forces applied to the system, while the dots denote the time derivatives. Applying the basic theorems of rigid body kinematics, we obtain the following recursive (Low et al., 2006):

$$\begin{aligned}
\vec{\omega}_i &= \vec{\omega}_{i-1} + \dot{q}_i\vec{e}_i \\
\vec{v}_i &= \vec{v}_{i-1} + \vec{\omega}_{i-1}\times\vec{r}_{i-1,i} + \vec{\omega}_i\times\vec{r}_{ii} \\
\vec{\alpha}_i &= \vec{\alpha}_{i-1} + \dot{q}_i\vec{\omega}_{i-1}\times\vec{e}_i + \ddot{q}_i\vec{e}_i \\
\vec{a}_i &= \vec{a}_{i-1} + \vec{\alpha}_{i-1}\times\vec{r}_{i-1,i} + \vec{\omega}_{i-1}\times(\vec{\omega}_{i-1}\times\vec{r}_{i-1,i}) \\
&\quad + \vec{\alpha}_i\times\vec{r}_{ii} + \vec{\omega}_i\times(\vec{\omega}_i\times\vec{r}_{ii})
\end{aligned} \tag{2}$$

where $\vec{\omega}_i$, $\vec{v}_i$, $\vec{\alpha}_i$ and $\vec{a}_i$ are the angular velocity, linear velocity of the center of mass, angular acceleration, and linear acceleration of the center of mass of the *i*-th link, respectively. The inertial force of the center of mass of the *i*-th link $\vec{F}_i$ and moment of the *i*-th link $\vec{M}_i$ can then be obtained by using Newton-Euler equations, respectively,

$$\vec{F}_i = m_i\vec{a}_i \tag{3}$$

$$\vec{M}_i = I_i\vec{\alpha}_i + \vec{\omega}_i\times I_i\vec{\omega}_i \tag{4}$$

4. Control Strategy of the Exoskeleton System

An important feature of the exoskeleton system, which is also the main difference between exoskeleton and biped robot, is the participation role of human in the process of control and decision-making. By introducing human as part of the control system, some intractable tasks for robots such as navigation, path planning, obstacle crossing and gait selection can be easily undertaken by the pilot instead of robot's complex artificial controller and vision system. However, two problems remain for the exoskeleton controller to solve: how to transfer the pilot's intention to the exoskeleton and how to keep the stability of the exoskeleton. Accordingly, the proposed control strategy can be divided into two parts, namely *Locomotion control* and *ZMP control.*

4.1 Locomotion Control

During the single support phase, the trajectory of the swinging foot determines the gait parameters such as step length, step height, etc. To ensure that the exoskeleton and the wearer can walk together, the trajectory of the exoskeleton's swing foot should trace that of the user in time. To do that, a mechanical linkage named *inner exoskeleton* is attached to the wearer operator (Low et al., 2006). Accordingly, the exoskeleton that is controllable and carrying payloads is named *outer exoskeleton.* The inner exoskeleton equipped with encoders is to capture the joint information of the pilot.

4.2 Control of the ZMP

If the ZMP of the exoskeleton is within the support area, it implies that the exoskeleton can keep the stability only by using the ground reaction force without adding any force to the user. In other words, the user will not feel any extra burden from the exoskeleton. Hence the

purpose of the ZMP control is to make sure the ZMP remain within the support polygon. From the definition of the ZMP, we have

$$(\vec{M}_G + \vec{M}_F) \cdot \vec{e}_X = 0 \tag{5}$$

$$(\vec{M}_G + \vec{M}_F) \cdot \vec{e}_Y = 0 \tag{6}$$

where $\vec{M}_G$ is the total movement of gravity forces with respect to ZMP, $\vec{M}_F$ is the total moment of inertial forces of all the links with respect to ZMP, while $\vec{e}_X$ and $\vec{e}_Y$ denote unit vectors of the X and Y axes of the absolute coordinate frame. Equation (6) can be further replaced with

$$\sum_{i=1}^{7}[(\vec{p}_i - \vec{p}_z) \times (G_i + \vec{F}_i) + \vec{M}_i].\vec{e}_Y = 0 \tag{7}$$

where $\vec{p}_z$ is the ZMP coordinates in the global coordinate frame, $\vec{p}_i$ is the position vector of the center of mass of the *i*-th link,

$$\vec{p}_i = \vec{p}^* + \sum_{j=1}^{i-1}(\vec{r}_{jj} - \vec{r}_{j,j+1}) + \vec{r}_{ii} \tag{8}$$

where $G_i = m_i g$ is the gravity force of link *i*, $\vec{p}^*$ is the position vector of joint 1 with respect to the global coordinate system. Substitute Eqs. (2), (3), (4), (8) into Eq. (7), one can obtain

$$\sum_{i=1}^{7} a_i \ddot{q}_i + \sum_{i=1}^{7}\sum_{j=1}^{7} b_{ij}\dot{q}_i\dot{q}_j + \sum_{i=1}^{7} c_i G_i = 0 \tag{9}$$

where the coefficients a_i, b_{ij} and c_i are the functions of the generalized coordinates q_i. The trajectories of q_1 to q_6 are determined by the signals measured from the pilot's legs, as mentioned before, while q_7 is determined according to Eq. (9) to ensure the ZMP in the support polygon. Such a ZMP is the desired ZMP. However, the actual ZMP may be different from the desired ZMP due to all kinds of reasons such as disturbance from the environment or error of the actuators. A footpad that can online measure the actual ZMP is thus designed.

4.3 Measurement of ZMPs

In a stable gait, during the single support phase, the CoP of the supporting foot is also the ZMP of the whole exoskeleton; during the double support phase, the relationship between the ZMP and the CoP is described by

$$X_p = \frac{f_{LZ}X_L + f_{RZ}X_R}{f_{LZ} + f_{RZ}}, \quad Y_p = \frac{f_{LZ}Y_L + f_{RZ}Y_R}{f_{LZ} + f_{RZ}} \tag{10}$$

where
ZMP= ($\boldsymbol{X}_p$, $\boldsymbol{Y}_p$, $\boldsymbol{Z}_p$): ZMP of the whole biped
CoP_L, = ($\boldsymbol{X}_L$, $\boldsymbol{Y}_L$,$\boldsymbol{Z}_L$): CoP of the left foot
CoP_R = ($\boldsymbol{X}_R$, $\boldsymbol{Y}_R$, $\boldsymbol{Z}_R$): CoP of the right foot
$\boldsymbol{f}_L$ = ($\boldsymbol{f}_{LX}$,$\boldsymbol{f}_{LY}$,$\boldsymbol{f}_{LZ}$): ground reaction force at CoP_L
$\boldsymbol{f}_R$ = ($\boldsymbol{f}_{RX}$, $\boldsymbol{f}_{RY}$, $\boldsymbol{f}_{RZ}$): ground reaction force at CoP_R

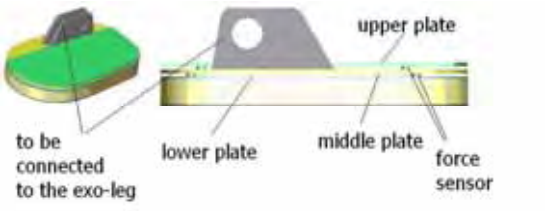

Figure 7. Design of the exoskeleton foot

To measure the ZMPs of the wearer and the exoskeleton, a footpad is designed as shown in Figure 7. The wearer's foot will be on the upper plate, and the exoskeleton leg will be connected to the middle plate. There are four force sensors between the upper plate and middle plate, the middle plate and lower plate, respectively. The sensors are distributed as shown in Figure 8. During the single support phase, Sensors 1-4 measure the ground reaction force under the human foot, and the ZMP coordinates of the human in the foot's local coordinate frame can be obtained according to

$$ZMP_h = \frac{\sum_{i=1}^{4} F_i r_i}{\sum_{i=1}^{4} F_i} \tag{11}$$

where $\boldsymbol{F}_i$ is the force measured by sensor i at the distance (r_i) from O, as denned in Figure 8. Sensors 5-8 measure the ground reaction force under the whole system (the human and the exoskeleton). Similarly, the ZMP of the whole system can be calculated by

$$ZMP_w = \frac{\sum_{i=5}^{8} F_i r_i}{\sum_{i=5}^{8} F_i} \tag{12}$$

The ZMP of the exoskeleton is on the radial distance from the human ZMP to the whole system's ZMP, and its position can be obtained by

$$ZMP_e = \frac{\sum_{i=1}^{4} F_i (r_w - r_h)}{\sum_{i=5}^{8} F_i - \sum_{i=1}^{4} F_i} + r_w \tag{13}$$

as we take the moment about the point of ZMPW,

$$(\sum_{i=5}^{8} F_i - \sum_{i=1}^{4} F_i)(ZMP_e - r_w) = \sum_{i=1}^{4} F_i (r_w - r_h) \tag{14}$$

in which r_h and r_w are the coordinates of the human's ZMP and the ZMP of the whole system (human plus exoskeleton), respectively, as shown in Figure 9. Note that the ZMP is expressed in terms of $\boldsymbol{X}$, $\boldsymbol{Y}$ coordinates. During the double support phase, instead of the ZMPs, the CoPs of each foot are obtained from Eqs. (11) - (13). By substituting those CoPs of the human and the exoskeleton into Eq. (10), respectively, ZMP of the human and that of the exoskeleton can be obtained accordingly.

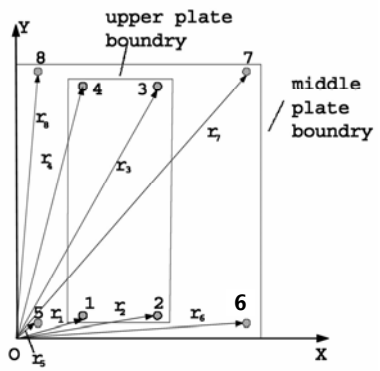

Figure 8. Location of the distributed sensors

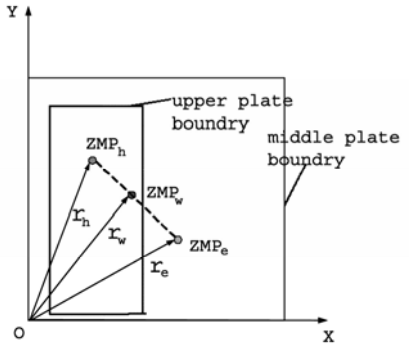

Figure 9. Relationship between the human ZMP and the exoskeleton's ZMP

4.4 Trunk Compensation

If the actual (currently measured) ZMP of the exoskeleton differs from the desired ZMP, trunk compensation will be applied to shift the actual ZMP to an appropriate position. Without losing generality, only motion in the sagittal plane during single support phase is discussed here. The trunk compensation in the frontal plane or during double support phase can be performed in the similar way. As shown in Figure 10, the actual ZMP differs from the desired ZMP in the direction of $\boldsymbol{X}$ axis by Δx. Note that the ground reaction force $\boldsymbol{F}_z$ acts on the exoskeleton can be derived from $F_z = \sum_{i=5}^{8} F_i - \sum_{i=1}^{4} F_i$. For simplicity, we assume that the action of the trunk joint k will not cause a change in the motion at any other joint. The system will then behave as if it was composed of two rigid links connected at trunk joint k, as depicted in Figure 10. The payload and the exoskeleton trunk as shown in the figure are considered as an upper part of total mass m and inertia moment $\boldsymbol{I}_k$ for the axis of joint k $(\text{as } I_k = I_c + ml_1{}^2)$. Point c is the mass center of the upper part, and the distance from k to $\boldsymbol{C}$ is denoted by l_1. The lower part, representing the sum of all the links below the trunk joint k, including another leg that is not drawn in the figure, is also considered as a rigid body, which is standing on the ground surface and does not move. The distance from $\boldsymbol{O}$ to k is denoted by l_2. Note that $\Delta \boldsymbol{T}_k$ stands for the correctional actuator torque, applied at joint k.

Assuming that the additional torque ΔT_k will cause change in acceleration of the upper part $\Delta\ddot{\beta}$, while velocities will not change due to the action of ΔT_k, $\Delta\dot{\beta} \approx 0$. Next the following equations are derived:

$$\Delta T_k = I_k \Delta\ddot{\beta} \tag{15}$$

$$F_z \Delta x = \Delta T_k + m l_1 l_2 (\cos\beta\cos\alpha + \sin\beta\sin\alpha)\Delta\ddot{\beta} \tag{16}$$

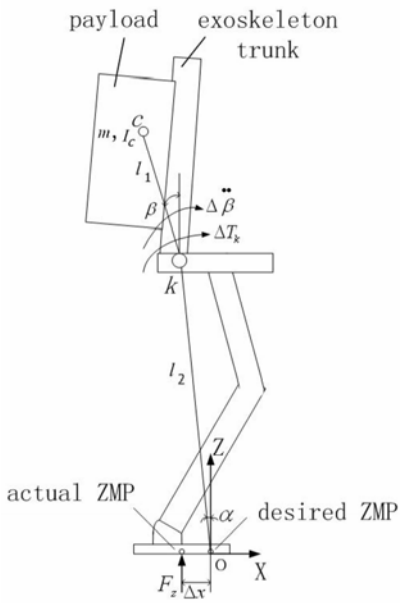

Fig. 10. Adjusting ZMP by trunk compensation

By virtue of Eq. (15), we have

$$\Delta\ddot{\beta} = \frac{\Delta T_k}{I_k} \tag{17}$$

Substituting Eq. (17) into Eq. (16), we obtain

$$\Delta T_k = \frac{F_z \Delta x}{1 + \frac{m l_1 l_2 (\cos\beta\cos\alpha + \sin\beta\sin\alpha)}{I_k}} \tag{18}$$

Taking into account that ΔT_k is derived by introducing certain simplifications, an additional feedback gain K_{zmp} is introduced into Eq. (18) as

$$\Delta T_k = K_{zmp} \frac{F_z \Delta x}{1 + \frac{m l_1 l_2 (\cos\beta\cos\alpha + \sin\beta\sin\alpha)}{I_k}} \tag{19}$$

where K_{zmp} can be determined by the feedback in the actual walking. Equation (19) shows how to drive the actual ZMP towards the desired ZMP by controlling the torque output of the trunk joint.

5. Simulation

It is necessary to verify a control algorithm using a software simulator before it is put into practice, because unsuccessful control method may cause great damages to the user or/and the exoskeleton. On the other hand, to develop a hardware exoskeleton with the desired physical capability, it is desired to clarify the required specifications of components in advance. An exoskeleton simulator, consisting of component parameters, is a useful tool to solve this problem. In this chapter, a human and an exoskeleton simulators are established using ADAMS (*Homepage of the Adams University*, Jan. 2005) and MATLAB (*MATLAB - the language of technical computing*, Jan. 2005) and walking simulations are performed to verify the control algorithms. Moreover, the moving range of each joint and the power needed by each actuator are analyzed.

5.1 Simulation Environment

To predict the physical biped (human/exoskeleton) motion, it is necessary to accurately formulate and solve the kinematic and dynamic equations of the mechanisms. However, the biped is a system with multiple bodies and many degrees of freedom. The analytical complexity of nonlinear algebraic equations of kinematics and nonlinear differential equations of dynamics makes it practically impossible to obtain closed-form solutions. On the other hand, there are some commercial dynamic software packages such as ADAMS, 3D Working Model, DADS, etc., whose usefulness has been illustrated in many areas. These software packages can automatically formulate the equations of kinematics and dynamics, solve the nonlinear equations, and provide computer graphics output of the simulation results (Haug, 1989). After compared with other commercially available simulation software, ADAMS is selected due to its high numerical accuracy. Another benefit of ADAMS is that it incorporates easily with control software packages such as MATLAB and MATLAB accepts user defined subfunctions. It is therefore possible to model detailed functions, define special constraints, and develop original control algorithms.

5.2 Exoskeleton Model

This section describes the kinematic structure of the human model. Figure 11 shows the human model established in ADAMS, and the human consists of legs, a waist, a trunk, and arms and a head. The CAD model adopts measured human data and parameters are set according to an adult with a 65 kg weight and 1.7 m height. The lengths of the leg's parts, which are crucial parameters of walking, are listed in Table 1. There are three degrees of freedom (DoF) in the hip joint, one in the ankle joint and one in the knee joint. There is also a DoF between the trunk and the waist. Also shown in Figure 11, an exoskeleton model is established, and a payload is carried by the exoskeleton. The links of the exoskeleton is parallel to those of the human, and the height of each joint (ankle, knee and hip) is equal to the corresponding one of the human. The exoskeleton model is set to have the same size and mass as those of the actual exoskeleton constructed. The mass of each part of the exoskeleton is listed in Table 2.

Height of Ankle	Length of Calf	Length of Thigh	Length of Foot	Width of Foot
80 mm	420 mm	440 mm	200 mm	100 mm

Table 1. Parameters of the human model's lower limbs

Foot and Ankle Joint	Calf	Thigh and Knee Joint	Waist Frame and Two Hip Joints	Back Frame and Linear Actuators
3 kg	1.68 kg	4.77 kg	9.54 kg	6.12 kg
Total	(3+1. 68+4.77)*2+9. 54+6.12= 34.56 kg			

Table 2. Mass of the exoskeleton

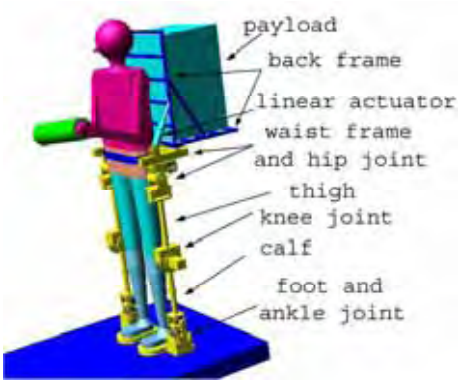

Figure 11. The NTU exoskeleton model

5.3 Walking Simulation

To run the walking simulation, there are three problems should be solved, namely contact model, locomotion control and trunk compensation control.

5.3.1 Contact Model

The reaction force between the feet and the ground strongly affects the behavior of the exoskeleton and human model. For example, if the impact force arising when the feet hit the ground is too large, the burden on joints of supporting the exoskeleton becomes large, and the exoskeleton will easily vibrate and become unstable. ADAMS adopts a spring-damper element to model the normal force between two contact objects. The IMPACT function activates when the distance between the first object and the second object falls below a nominal free length (x_1), that is, when two parts collide. As long as the distance between the first object and second object is greater than x_1, the force is zero. The force has two components, a spring or stiffness component and a damping or viscous component. The stiffness component is proportional to the stiffness k, and is a function of the penetration of the first object within the free length distance from the second object. The stiffness component opposes the penetration. The damping component of the force is a function of the speed of penetration. The damping opposes the direction of relative motion. To prevent a discontinuity in the damping force at contact, the damping coefficient is, by definition, a cubic step function of the penetration. Thus, at zero penetration, the damping coefficient is always zero. The damping coefficient achieves a maximum, c_{max}, at a user-defined penetration, d. The equation defining IMPACT is:

$$IMPACT = \begin{cases} \max(0, k(x_1 - x)^e - STEP(x, x_1 - d, c_{\max}, x_1, 0) * \dot{x}) & : x < x_1 \\ 0 & : x > x_1 \end{cases}$$

To absorb the shock when the exoskeleton's feet contact the ground, we propose to install elastomeric material on the feet of the exoskeleton. This situation can be simulated to investigate the effect of this measure on the ground reaction force. Figure 12 shows the two ground reaction force curves of the exoskeleton's right foot corresponding to the two walking with different footpad stiffness. It can be seen that with the stiffness decreasing, not only the impact force is smaller, the force curve is also more smooth. The simulation demonstrates that the elastomeric material can low-pass filter shock impulse and reduce the impact, therefore allowing the structure interacting with the environment at a pretty high speed.

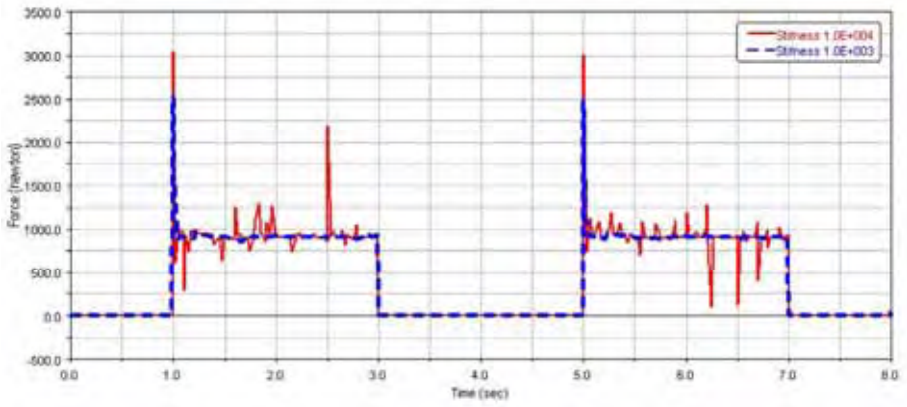

Fig. 12. Effect of foot's stiffness on the contact force

5.3.2 Locomotion Control

The human motion capture data (HMCD) is used to generate human-like walking motions of the human and exoskeleton models. As mentioned above, the human model's parameters are set according to an adult. To obtain the HMCD, encoders are attached to the joints of the wearer's lower limbs and the walking motion is thus captured. The human limbs are soft due to the muscles and tendons, while the model's limbs are firm. Besides, human has much more DoFs than the model. Hence the human motion data cannot be used directly to drive the human model. The recorded data is processed and edited based on the inverse kinematics of the human model and interpolated using Akima spline before being input into the ADAMS. Adams will calculate the human model's joints move according to those trajectories (Low et al., 2006).

5.3.3 Trunk Compensation

As mentioned earlier, the control of the exoskeleton is divided into leg trajectories control and ZMP control. In this simulation, the exoskeleton model's leg trajectories is controlled by human model's leg trajectories. To keep the exoskeleton walk stably, trunk should be controlled according to the ZMP of the exoskeleton. The trunk compensation function is implemented in MATLAB.

During the simulations using the MATLAB toolbox Simulink, at each time interval, the angular values, joint velocities and accelerations are sent to MATLAB, and those data

is used by a trunk compensation module to calculate the torque needed at the trunk joint and such a torque will be applied in Adams so that the exoskeleton model can walk stably. Figure 13 shows the torque applied to the exoskeleton trunk joint for the changing masses of the load (5 kg and 20 kg).

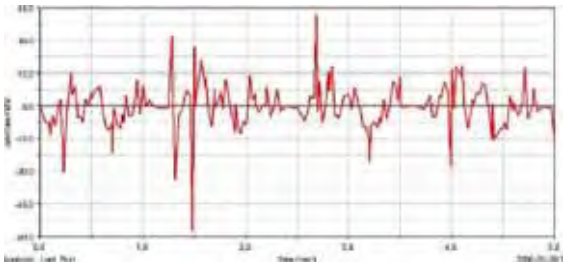

mass of load = 5kg

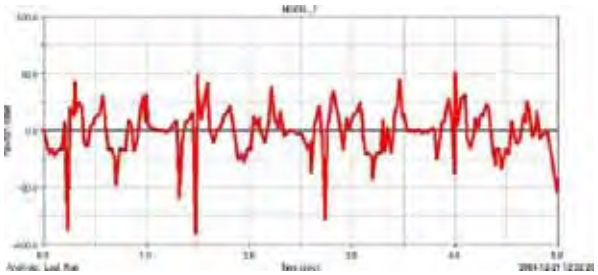

mass of load - 20kg

Figure 13. Torque at the trunk joint

5.4 Simulation Results

Without losing generality, we present only the results of the joints of the exoskeleton's right leg. The 30-kg payload is assumed and used in our simulation.

Ankle

Figure 14 shows the data of the ankle flexion/extension torque. The ankle torque is almost zero when the right leg is in swing phase. The torque is largest when the right foot is in its heel off phase. The instantaneous ankle mechanical power is calculated by multiplying the joint angular velocity and the instantaneous joint torque (Figure 14), as shown in Figure 15

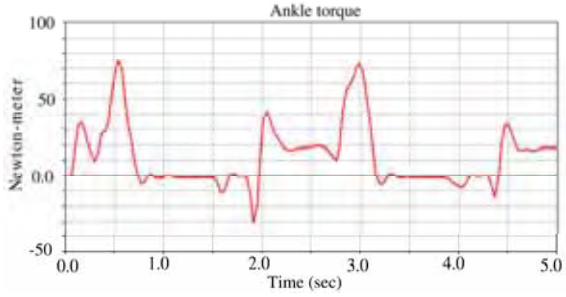

Figure 14. Ankle flexion/extension torque

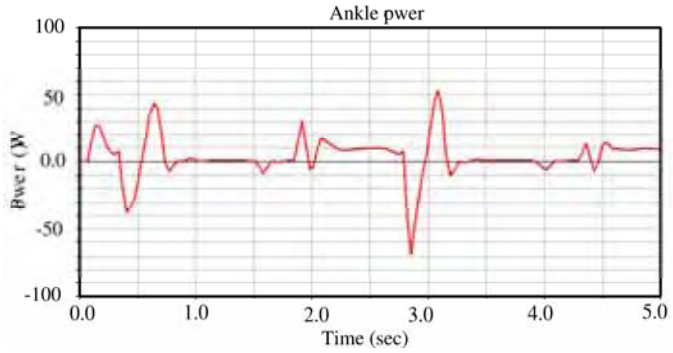

Figure 15. Ankle instantaneous mechanical power

Knee

The knee buckles momentarily in early stance to absorb the impact of heel strike then undergoes a large flexion during swing. This knee flexion decreases the effective leg length, allowing the foot to clear the ground when swinging forward. Although the walking knee flexion is up to approximately 0.6 rad or 34°, the human has significantly more flexibility-up to 160° when kneeling (Kapandji, 1987). The LEE knee motion range was set to from 0° to 110°. Figure 16 shows the data of the knee flexion/extension torque. The highest peak torque is in early stance (from heel contact to foot flat). Figure 17 shows the instantaneous mechanical power required by the knee joint.

Hip

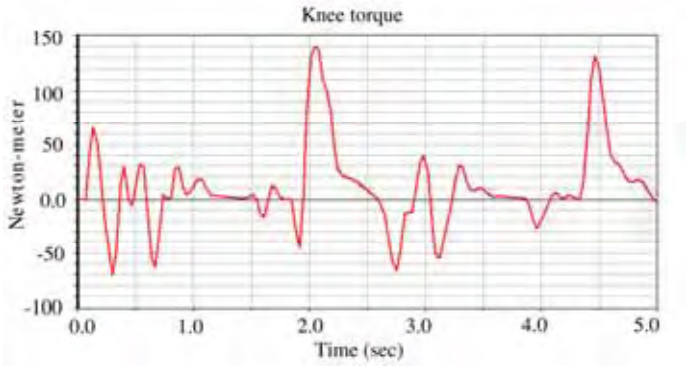

Figure 16. Knee flexion/extension torque

The thigh moves in a sinusoidal pattern with the thigh flexed upward at heel contact to allow foot contact the ground in front of the person. This is followed by an extension of the hip through most of stance phase and a flexion through swing. An average person can flexion reaches 90° with the knee extended. With the knee flexed, flexion can reach up to 120° or even beyond. When the knee is in extension, extension of the hip reaches 20° , when the knee is flexed, extension of the hip reaches 10°. The LEE hip angle is designed to 10° extension and 80° flexion. Figure 18 shows the data of the hip flexion/extension torque and Figure 19 shows the instantaneous mechanical power required by the hip joint.

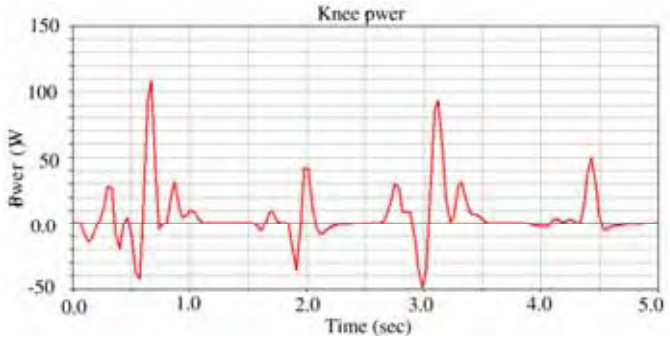

Figure 17. Knee instantaneous mechanical power

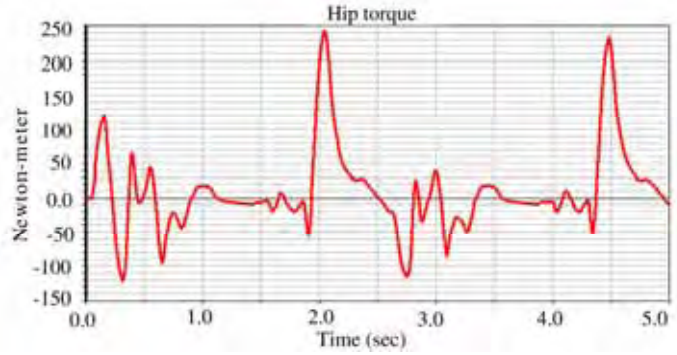

Figure 18. Hip flexion/extension torque

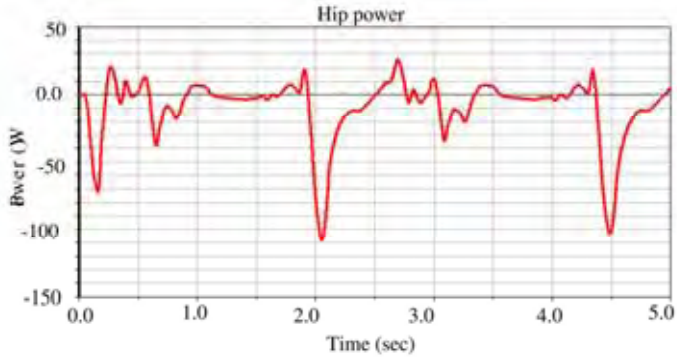

Figure 19. Hip instantaneous mechanical power

6. Design and Construction of Prototypes

This section introduces the design of the lower extremity exoskeleton system, including the inner lower exoskeleton and the outer lower exoskeleton.

6.1 Inner Lower Exoskeleton

The inner exoskeleton is used to attach the encoders to the human limbs. It exists between the human limbs and the outer lower exoskeleton and its weight is carried by the user. Hence, it must be as light and compact as possible. The conceptual design is shown in Figure 20. A minimum protrusion is achieved by designing the brackets to allow the tip of the encoder spindle to actually touch the surface of the user. This feat was achieved by the use of a larger but extra thin bearing which allows the rotary encoder to reside within the bearing itself. In this design, linkages are separated from the encoder housing. This modular concept of the housing allows the same housing unit to be repeated for the hip unit, the knee unit and the ankle unit. This modular design also cuts down on both design and manufacturing time. To position the rotary encoder brackets firmly on the respective bodily positions on the lower extremity of the human body, a need arise to design a harness system which is versatile, reliable, light and durable. Nylon being a material that economical, durable and easily worked with was selected as the choice material for the harness. For the harness used in the knee brackets, Velcro was chosen due to its ability to conform readily to the shape of the user's thigh. Also, with the Velcro, we can easily compensate for slight variations the variant dimensions of the various user thigh heights without having to adjust the buckle position.

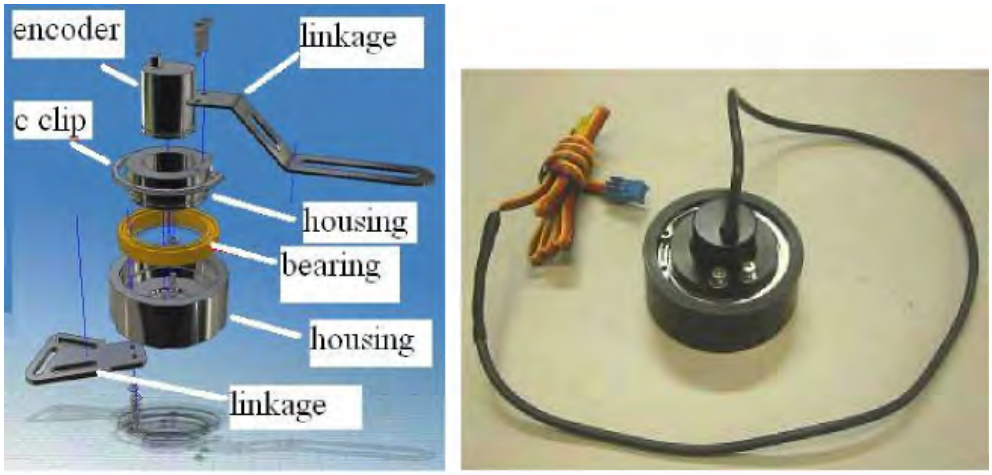

(a) (b)

Figure 20. The encoder bracket

6.2 Outer Lower Exoskeleton

The outer lower exoskeleton (OLE) provides the mechanical hardware means for the exoskeleton system. Therefore, it must be made of structures and mechanisms strong enough to carry a load and travel by itself. The OLE is a powered lower exoskeleton, which means that it is to be worn by the user from the user's waist down to the user's feet. The OLE has to be able to carry its own weight as well as a payload and should not hinder the walking movements of the user. The fully OLE CAD model is shown in Figure 21, while Figure 22 shows the overview of the whole OLE prototype.

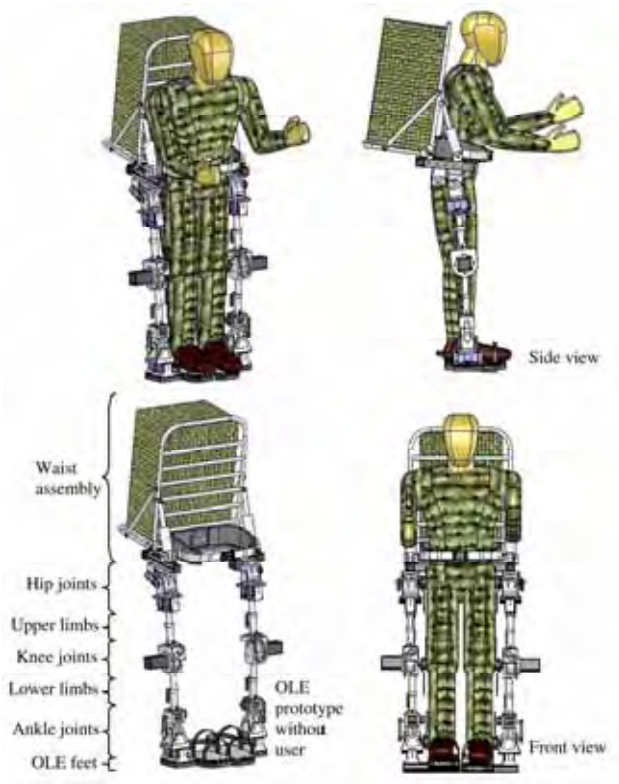

Figure 21. The overall design

Figure 22. Photos of the OLE prototype

7. Walking Implementation of the Exoskeleton

The important function of the inner exoskeleton is to read necessary input data from the operator. These data will be analyzed, and transformed into corresponding commanded signals for the outer exoskeleton using certain mapping algorithms, and then transferred to the outer exoskeleton through a communication means. An operation of a dynamic system is called a real-time operation if the combined reaction- and operation-time of a task is shorter than the maximum delay that is allowed. When the human operator performs one action, the OLE should react correspondingly as fast and precise as possible, i.e., the OLE should be controlled real-time.

7.1. Real-Time Operating System Used in this Work

A Real Time Operating System or RTOS is an operating system that has been developed to serve for real-time applications. Some examples of RTOSes are QNX, RMX, RT-11, LynxOS, MicroC/OS-II, etc. In this work, xPC Target toolbox in MATLAB is employed (Mosterman et al., 2005). xPC Target provides a high-performance, host-target prototyping environment that enables developers to connect system simulation models (which can be created using Simulink and Stateflow toolbox from MATLAB) to physical systems and execute them in real time on PC-compatible hardware. xPC Target provides comprehensive software capabilities for rapid prototyping and hardware-in-the-loop simulation of control and signal processing systems. It can also enables users to add I/O interface blocks to their models (system models and controller designs, etc.), automatically generate code with R,eal-Time Workshop and Stateflow Coder, and download the code to a second PC running the xPC

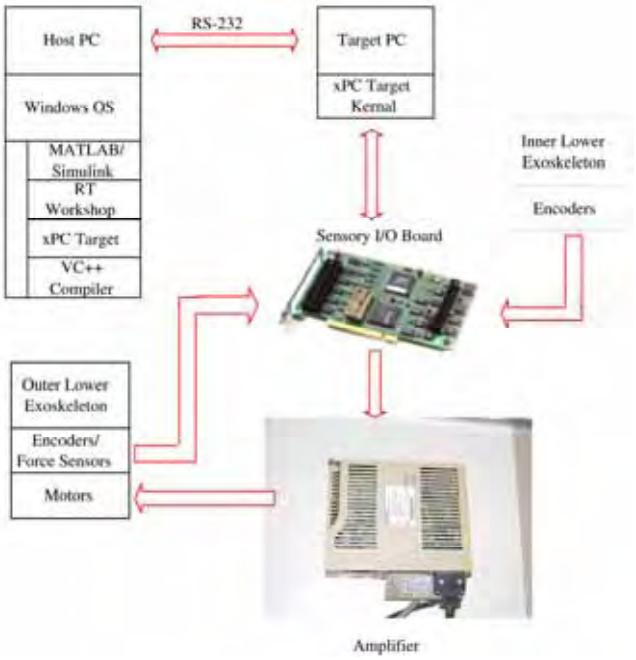

Figure 23. Control system architecture of the exoskeleton system

Target realtime kernel. This capability to rapidly produce code directly from verified system results allows many different techniques to be tried on hardware in a more convenient way compared to other software, operating systems. Developers, who use the other systems, most of the time, have to deal with low-level programming languages directly. These kinds of low-level programming languages are somewhat not very efficient in the sense that they take developers long time to deal with coding and debugging. The system includes softwares such as Matlab, xPC Target etc., which run in the PCs, and I/O boards that receive commands from xPC Target and control the motors via amplifies. The overall architecture of the host-target hardware-in-the-loop exoskeleton control system established in this work is shown in Figures 23 and 24.

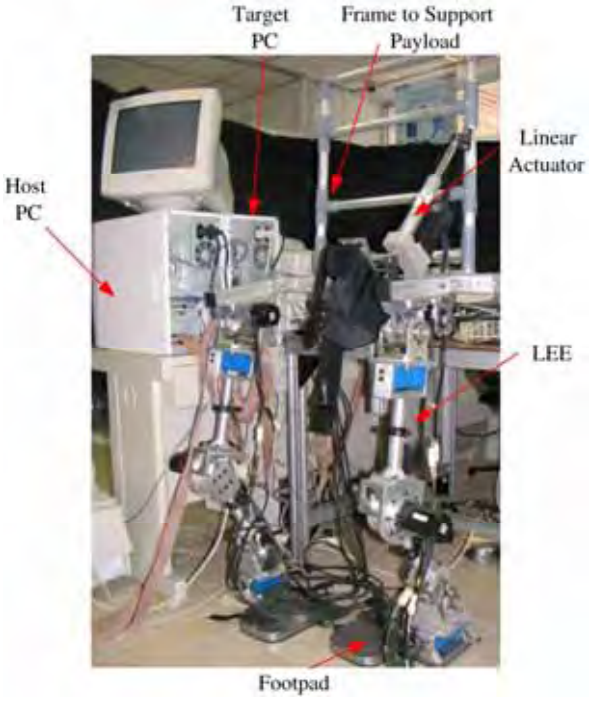

Figure 24. Set-up of developed control system

7.2 Control of the Developed Exoskeleton

Quite often, robots have the two lowest control levels. The tactical level generates the trajectories of each DoF, which perform the desired functional movement, while the executive level executes these trajectories by means of appropriate actuators, incorporated in each DoF. The two upper control levels are generally recognized as intelligence level. R.obots with the two upper levels such as ASIMO *(Asimo. the humanoid robot by Honda,* Dec. 2003; Hirose, Haikawa, Takenaka, & Hirai, 2001), QRIO *(QRIO. the humanoid entertainment robot by SONY,* Dec. 2003), HRP-2 (Kanehiro et al., 2003; Kaneko et al., 2004), etc. can walk on a terrain of unknown profile. While those robots walking in a known environment whose trajectories of each link can be pre-defined off-line do not need the two upper levels. In

stead of artificial intelligence, the highest level of the exoskeleton's control structure is implemented by the human user. The user recognizes the obstacles using his/her natural sensors, decide where to go and how to go. The second level is to transfer the human intention into the exoskeleton's controller and the controller divides the imposed operation into elementary movements. The two lowest control levels are similar to those of the robots. In other words, the exoskeleton can be seen as a robot integrated with the human intelligence. Figure 25 shows the snapshots of a trial with a patient whose left leg is very weak after strokes. The patient confirmed that the exoskeleton's leg responds well and he could hardly feel any extra burden.

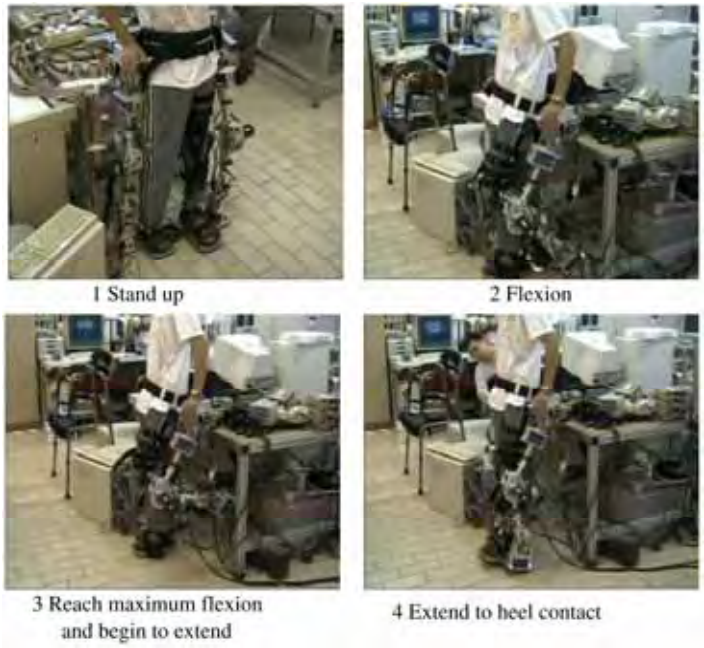

Figure 25. Exoskeleton trial with post-stroke patient

7.3 Measurement of the ZMP

As mentioned earlier, the ZMP has been introduced into the control strategy for stable exoskeleton walking. In this section, the experiment of measuring the human ZMP during walking is presented. In this experiment, a human walks as described in Figure 26. First, the human stands up, the width between his left foot and right foot is 300 mm. He then walks forward, and his right foot moves first, from position Rl to R2. Next, his left foot moves from position LI to position L2. Thirdly, his right foot moves from position R2 to position R3. At last, his left foot moves from position L2 to position L3 and he recovers stand posture. The step length is 300 mm. There are four force sensors placed below the human each foot. The reading in Figure 27 shows the timing of the ground reaction force below the two feet. At the first second, the human begins to walk. From the fifth second the human recovers stand posture. Using Eqs. (10) and (11), the ZMP of the human is calculated, as shown in Figure 28. Figure 27 and Figure 28 show that when the human begins to walk, the ground reaction

force below his right foot decreases while the force below his left foot increases. The ZMP shifts from the middle of two feet to the left foot, i.e., the supporting foot area. During the walking, the ZMP shifts between the two feet. At last, when the human recovers stand posture, the ZMP stays between the two feet.

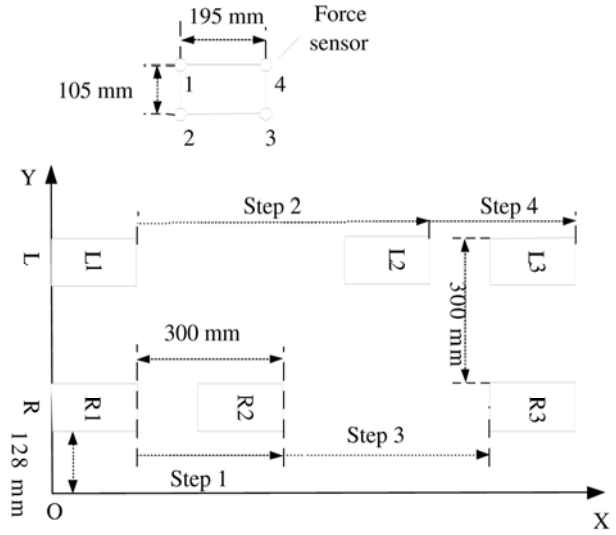

Figure 26. Steps of the walking experiment

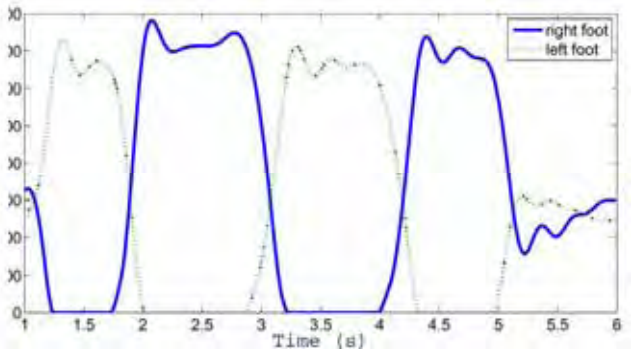

Figure 27. Timing of the ground reaction force below the two feet

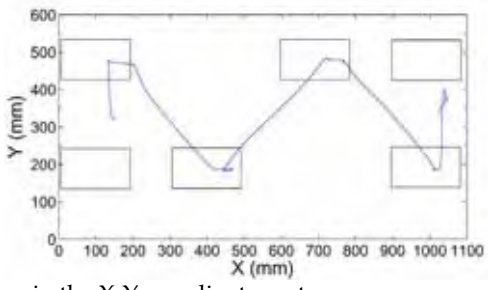

Figure 28. ZMP trajectory in the X-Y coordinate system

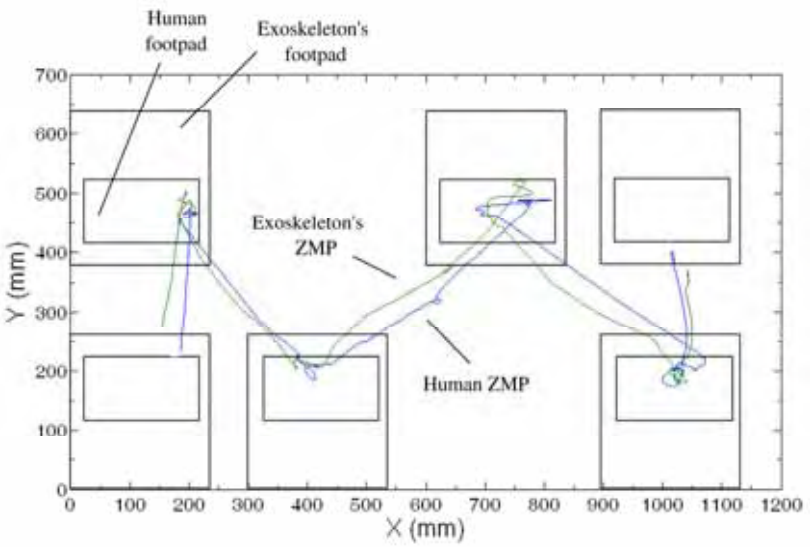

Figure 29. Human and exoskeleton's ZMP trajectories in the X-Y coordinate system

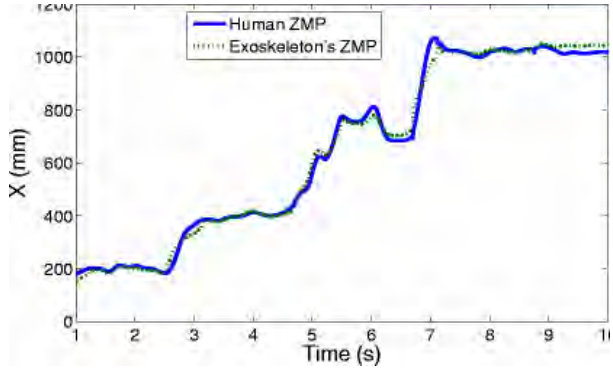

Figure 30. X coordinate of the human and exoskeleton ZMPs with respect to time

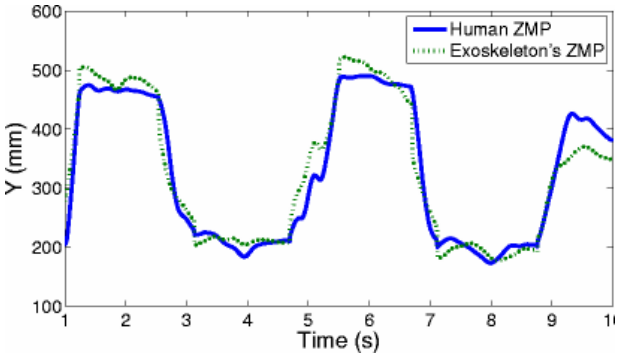

Figure 31. Y coordinate of the human and exoskeleton ZMPs with respect to time

7.4 Exoskeleton's Walking Experiments

An online balancer is added into the control scheme (Low et al., 2006). One more I/O board is employed, which reads the encoder of the trunk joint, signals from force sensors and control the actuator of the trunk joint. The balancer module reads the current joint angles and measured human ZMP then calculates the desired OLE's ZMP. If the measured OLE's ZMP differs from the desired one, suitable command signal will be applied to the actuator of the trunk joint and trunk compensation will shift the actual ZMP toward the desired position, as described previously. The ZMP will stay within the supporting area and the OLE will walk stably. A walking experiment is performed to check the balancer module. The walk procedure is similar to that in Figure 26. Figure 29 shows human and exoskeleton's ZMP trajectories in the *X*-*Y* coordinate system. This figure shows that the ZMP is adjusted during single support phase and the ZMPs are always kept in support area. Hence the exoskeleton can walk with the user stably. To see the relationship between the human ZMP and exoskeleton's ZMP more clearly, Figures 30 and 31 show the *X* and *Y* coordinates of the human and exoskeleton ZMPs with respect to time, respectively. These figures show that in *X* direction, the exoskeleton's ZMP is close to the human ZMP due to the trunk compensation, which ensures that the exoskeleton can walk stably following the human. In *Y* direction, the distance between exoskeleton's ZMP and the human ZMP is bigger. This is because the exoskeleton's footpad is much wider than human footpad (see Figure 29), therefore the allowable range of the exoskeleton's ZMP in *Y* direction is bigger. More experiments are performed including walking forward and backward with a payload of 20 kg. Figure 32 shows some snapshots of one of those experiments.

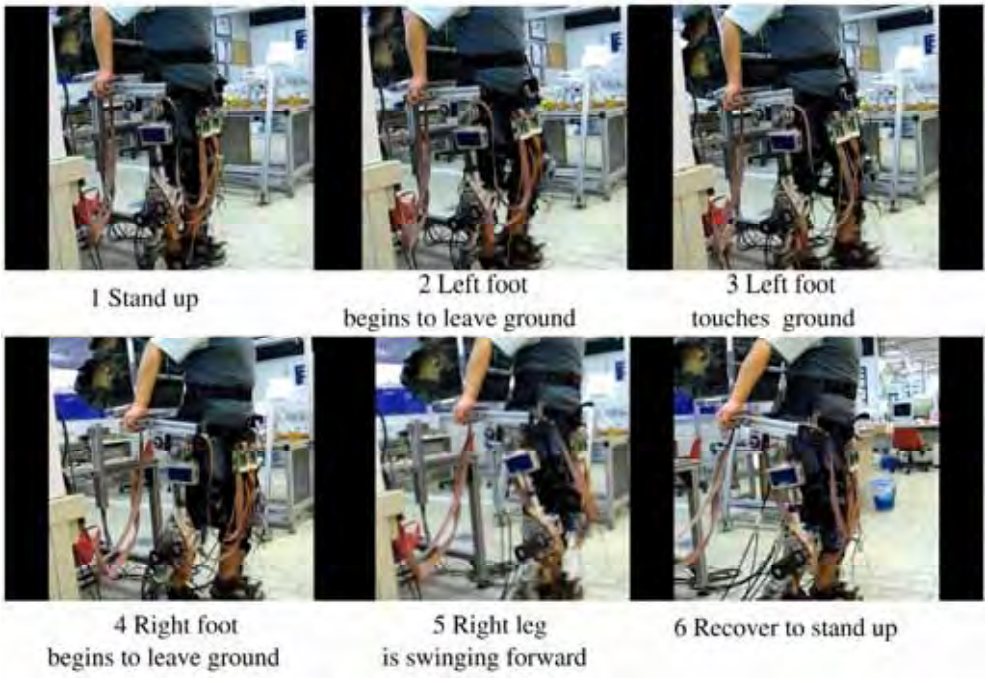

Figure 32. Snapshots of a walking test

8. Conclusion and Recommendations

8.1 Conclusion

This chapter has presented the development and control of a wearable lower exoskeleton system for augmentation of human walking ability, which incorporates human as the integral part of the control system and can relieve humans physical fatigue caused by excessive walking and heavy payloads. In this work, xPC Target, together with other toolboxes from MATLAB have been used so as to provide a real-time operating system and an integrated development environment for controlling the exoskeleton. Real-time control of the exoskeleton is implemented in this environment. At last, walking experiments are performed and demonstrated.

8.2 Future Work

The first prototype is only a test bed to verify the control algorithms. It looks bulky and rough. Though it has been verified that it can walk, there are some topics need to improve before one will see a reliable and useful exoskeleton that can effectively enhance humans strength and endurance. Another area of improvement may be the addition of more passive joints to the OLE prototype. These passive joints may be spring loaded such that it allows for passive movements without affecting the structural characteristics of the OLE. Examples of passive joints can be at positions like the feet where the passive joint can allow the bending of the OLE foot when walking. This will pertain to the users extension of the toes while walking. This addition of passive joints at the OLE feet will enable the OLE to be able to reciprocate the human movements better and at the same time, allow the user to have a more natural walking gait while wearing the OLE. Other areas where passive joints can be added are the hip joints and the ankle joints to allow them rotate. Now it is the inner exoskeleton who senses the user movements. However, the inner exoskeleton increases the distance between the user and the OLE. They can be replaced with goniometers *(BIOPAC systems. Inc.,* n.d.), which are more compact and light. Besides, human joints are not simple pin joints but complex joints with a changing instantaneous center of rotation. Compared to the hard linkages of the inner exoskeleton, goniometer has a telescopic end block that compensates for changes in distance between the two mounting points as the limb moves. The gauge mechanism allows for more accurate measurement of polycentric joints. To save energy and consequently reduce the size of the power source (e.g. batteries) carried by the OLE, ways to help decrease the torque required at the OLE joints could be developed. Such torque compensation mechanisms are not easy to construct, especially on the OLE. Issues like the amount of torque that will be reduced versus the weight increased by the addition of such a mechanism are widely debatable. Also, such a mechanism should not hinder the movements of the user or the OLE. With the addition of such torque compensation mechanisms, the controlling of the actuators will become more complicated. This is because of the additional parameters to controlling the torque output of the actuators. Nevertheless, a few torque compensation mechanisms can be a possible solution for the OLE. Firstly, in the development of the Saika-4 by Tohoku University (Shirata, Konno, & Uchiyama, 2004), a method of torque compensation was mentioned. Using a stainless-steel wire and a contrive spring layout, the mechanism is able to compensate without depending on joint angles. This is important as methods that depend on joint angles compensate with changing forces at every joint angle position. This increases the robustness of the control of the system. The mechanism in Saika-4 is reported to be able to reduce the torque requirements of the motors

at the robot joints because the robot legs always tend to return to the initial standing position by the spring force provided in the mechanism.
By virtue of the inner-outer exoskeleton systems, the proposed assistive gait device has been developed and tested initially for strength endurance and rehabilitation. The extension of the present study is currently applied to the rehabilitation of people with SCI (spinal cord injury) and post-stroke.

9. Acknowledgements

The authors would like to thank Miss Yunyun Huang, Mr. Tien-Boon Tan, Mr. Sui-Nan Lim, Mr. Tze-Kuang Ng, and Mr. Rene Wachter for their assistance in programming and experiments. Also, the help of Mr. Leong-Yeo Wai on the word processing is greatly appreciated. This research is supported by Research Grant MINDEF-NTU/02/01, a grant from the Ministry of Defence, Singapore. Robotics Research Center of the Nanyang Technological University provides technical helps, space and facilities.

10. References

Low K. H. and Yin Y., An integrated lower exoskeleton system towards design of a portable active orthotic device, *International Journal of Robotics and Automation*, 22 (1), pp. 32-42.

Berkeley robotics laboratory. (http://bleex.me.berkeley.edu/), Dec. 2004.

Exoskeletons for human performance augmentation projects. (http://www.darpa.gov/dso/thrust/md/Exoskeletons), 2002, Dec.

Guizzo, E., & Goldstein, H. The rise of the body bots. *IEEE Spectrum*, 42-48. 2005, Oct.

Haug, E. J. *Computer aided kinematics and dynamics of mechanical systems*. vol. 1: basic methods. Allyn & Bacon, Inc. 1989

Hembree, A. *Armor: the things they'll carry*. Wired News Online. (http://www.wired.eom/news/culture/0,1284,41216,00.html) 2001, Jan.

Hirose, M., Haikawa, Y., Takenaka, T., & Hirai, K. *Development of humanoid robot ASIMO.* 2001.

Homepage of the Adams University. (http://university.adams.com/tutorials.htm) Jan. 2005.

Kanehiro, F., Kaneko, K., Fujiwara, K., Harada, K., Kajita, S., Yokoi, K., et al. *The first humanoid robot that has the same size and that can lie down and get up*. 2003, Sep.

Kaneko, K., Kanehiro, F., KajitaK, S., Hirukawa, H., Kawasaki, T., Hirata, M., et al.. *Humanoid robot HRP-2*. 2004.

Kapandji, I. A. (1987). *The physiology of the joints* (5th ed., Vol. 2). Edinburgh London Melbourne and New York: Churchill Livingstone. (Translation of: Physiologic articulaire. v. 1. Upper limb - v. 2. Lower limb - v. 3. The trunk and the vertebral column (2nd ed., 1974))

Kasaoka, K., & Sankai, Y. *Predictive control estimating operator's intention for stepping-up motion by exoskeleton type power assist system HAL*. 2001, Oct..

Kawamoto, H., & Sankai, Y. *Comfortable power assist control method for walking aid by HAL-3*. 2002, Oct.)

Kazerooni, H., Racine, J.-L., Huang, L., & Steger, R. *On the control of the berkeley lower extremity exoskeleton* (BLEEX). 2005, Apr.

Low, K. H., Liu, X., Goh, C. H., & Yu, H. Locomotive control of a wearable lower exoskeleton for walking enhancement. *Journal of Vibration and Control*, 12(12), 1311-1336. 2006.

Low, K. H., & Yin, Y. An integrated lower exoskeleton system towards design of a portable active orthotic device. *International Journal of Robotics and Automation*, 22(1) in press. 2007.

Marchese, S., Muscato, G., & Virk, G. S. *Dynamically stable trajectory synthesis for a biped robto during the single-support phase*. Como, Italy. 2001, Jul.

Mavroidis, C. Smart portable rehabilitation devices. *Journal of NeuroEngineering and Rehabilitation*, 2(18), 8 pages. 2005.

Asimo, the humanoid robot by Honda. (http://www.honda.co.jp/ASIMO), Dec. 2003.

BIOPAC systems, Inc. (n.d.). (http://biopac.com/fr_prod.htm)

MATLAB - the language of technical computing. (http://www.mathworks.com/products/matlab/), Jan. 2005.

QRIO, the humanoid entertainment robot by SONY. (http:// www. sony.net/Sony Info/QRIO/story/index_nf. html), Dec. 2003.

RoboWalker. (http://yobotics.com/robowalker/robowalker.html), Dec. 2003.

Mosterman, P., Prabhu, S., Dowd, A., Glass, J., Erkkinen, T., Kluza, J., et al. *Handbook on networked and embedded systems.* In D. Hristu-Varsakelis & W. S. Levine (Eds.), (chap. Section 3.4: Embedded Real-Time Control via MATLAB, Simulink, and xPC Target). Birkhauser, Boston. 2005.

Powered-suit gives aged a leg up. (http://newpaper.asia!.com.sg/top/story/0,4136,31694,00.html), Dec. 2003

Powered suit HAL (Hybrid Assistive Leg). (http://sanlab.kz.tsukuba.ac.jp/HAL/indexE.html), Dec. 2003.

Shirata, S., Konno, A., & Uchiyama, M. Design and development of a light-weight biped humanoid robot Saika-4-, 2004, Sep.

Tomohiro Hayashi, H. K., & Sankai, Y. *Control method of robot suit HAL working as operator's muscle using biological and dynamical information*. 2005, Aug.

Vukobratovic, M., Borovac, B., Surdilovic, D., & Stokic, D. T*he mechanicl systems design handbook*: modeling, measurement, and control. In (chap. Humanoid Robots). Osita D.I. Nwokah, Yildirim Hurmuzlu, Southern Methodist University Dallas, Texas. 2001.

Vukobratovic, M., & Juricic, D. *Contribution to the synthesis of biped gait*. 1969.

Wakefield, J. *US looks to create robo-soldier*. BBC News Online. (http://news.bbc.co.Uk/2/hi/science/nature/1908729.stm), 2002, Apr.

Whittle, M. W. *Gait analysis*: an introduction. Oxford; Boston: Butterworth-Heinemann. 1991.